

LARGE-AMPLITUDE MEMS ELECTRET GENERATOR WITH NONLINEAR SPRING

Daigo Miki, Makoto Honzumi, Yuji Suzuki, and Nobuhide Kasagi
Dept. of Mechanical Engineering, The University of Tokyo, Tokyo, Japan

ABSTRACT

A MEMS electret generator with nonlinear spring has been developed for energy harvesting applications. By using hybrid high-aspect-ratio parylene springs, a large-amplitude oscillation over 1.0 mm_{p-p} has been obtained in a broad frequency range of 46-73 Hz. By using our mechanical model of the nonlinear spring, we have confirmed that the model can mimic frequency response of the mass-spring system. With the aid of electrostatic levitation mechanisms for keeping the air gap, power output of 1.0 μW has been obtained at 63 Hz.

INTRODUCTION

Micro power generation system from structural vibrations attracts much attention for its use in network nodes such as structural health monitoring systems and automotive sensors [1-2]. Since the frequency range of vibration existing in the environment is tens of Hz, electrostatic power generators using electret [3-6] should have higher output power than electromagnetic ones.

We have recently developed a high-performance electret material based on amorphous perfluorinated polymer CYTOP [7] and obtained extremely-high surface charge density of 1.5 mC/m². Edamoto et al. [8] microfabricated a prototype of electret generator with parylene high-aspect-ratio springs [9], which allow low resonant frequency and large amplitude. However, in our previous prototype, large amplitude is obtained only at the resonant frequency, and thus its performance should be deteriorated when the oscillation frequency varies.

In the present study, we develop a MEMS electret generator with hybrid parylene springs to realize nonlinear mass-spring systems and examine its performance under different operation conditions.

DESIGN OF ELECTRET GENERATOR

In electret generators, power output is increased with decreasing the air gap in between the electret and the counter electrode. Thus, the gap control is crucial to keep the narrow gap yet to avoid pull-in due to large electrostatic attraction force in the vertical direction. In the present design, patterned electrets are formed both on the seismic mass and the bottom substrate for electrostatic repulsion force between opposed patterned electrets [10]. In addition,

the dual-phase arrangement of electrodes [11] is employed in order to reduce the magnitude of horizontal unidirectional electrostatic force.

Figure 1 shows a schematic of the micro electret generator designed in the present study. The top substrate consists of a Si mass supported with parylene high-aspect-ratio springs [9], of which spring constant is 10 N/m. A fixed-free secondary spring, of which spring constant is 20 N/m, is also formed on both sides of the Si frame in order to realize nonlinearity of the hybrid spring systems. The secondary spring is in contact with the Si mass for the amplitude larger than 0.5 mm. The air gap between the substrates is defined with micro beads.

Dimension of the device and the mass is respectively 18.5 x 16.5 mm² and 11.6 x 10.2 mm². Designed value of the resonant frequency is 63 Hz. When 1 G vibration is imposed at the resonant frequency, power output estimated with the numerical simulation [11] is 10 μW for the surface voltage of -620 V.

MEMS FABRICATION PROCESS

Fabrication process of the electret generator is shown in Fig. 2. For the top substrate with a seismic mass, the process starts with a 400 μm-thick 4" Si wafer with 1.5 μm-thick thermal oxide. The oxide layer on the front side is patterned with BOE for the etch mask of DRIE, and 20-μm-wide 350-μm-deep trenches are etched into the substrate (Fig. 2a). The trenches are employed as the mold for parylene springs as well as boundaries of the Si mass and the frame to be left. Then, bottom Cr/Au/Cr electrodes are evaporated on the backside and patterned with standard lithography process, followed by spin-on

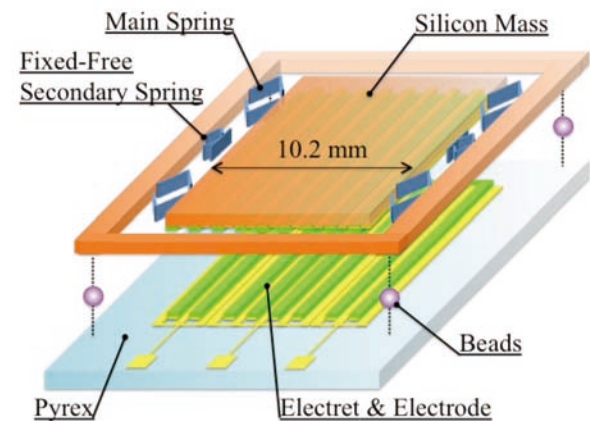


Figure 1. Schematic of the micro electret generator.

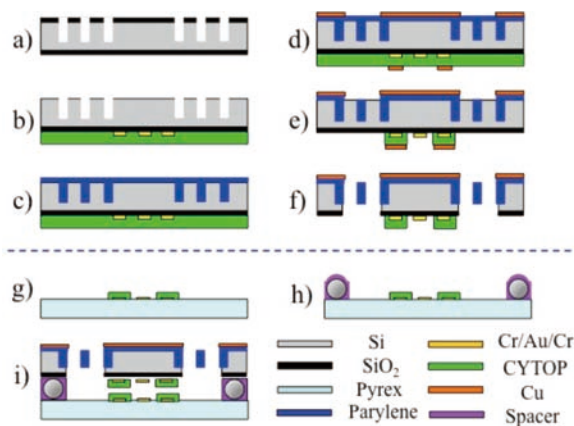


Figure 2. Fabrication process of the electret generator.

15- μm -thick CYTOP (CTL-809M) films and curing at 185 °C for 1.5 hours (Fig. 2b). Next, 15- μm -thick parylene-C is deposited on the front side and etched back with O₂ plasma. This is followed by the second parylene-C deposition to fully refill the trenches (Fig. 2c). After the metal mask on the CYTOP and parylene films is patterned (Fig. 2d), these films are etched with O₂ plasma (Fig. 2e). Finally, the bulk Si in between the Si mass and frame is etched away with XeF₂, and the structures are released (Fig. 2f). For the bottom Pyrex substrate, Cr/Au/Cr electrodes and 15- μm -thick CYTOP film are patterned with the similar procedure (Fig. 2g).

After these processes, charges are implanted into the CYTOP electret using corona discharge for 3 minutes at 120 °C, which is slightly higher than the glass transition temperature of CYTOP. The needle and grid voltages are respectively -8 kV and -600 V. The micro beads, of which diameter is well defined, are mixed with epoxy adhesive and applied to the Pyrex substrate (Fig. 2h) as the spacer. Finally, the top Si and the bottom Pyrex substrates are aligned and bonded (Fig. 2i). The air gap between the substrates is 70 μm .

Figures 3-5 show photographs of the generator prototype thus fabricated. The seismic mass is supported with 20- μm -wide high-aspect-ratio parylene springs. The fixed-free secondary spring is shown in Fig. 4c. The width of the patterned electret and electrode is 480 μm . On the backside of the top substrate, 8 stripes of patterned electrets are formed for each phase of the generator (Fig. 4a). On the bottom Pyrex substrate, patterned electrodes as well as pads for external connection are formed (Fig. 5a). Magnified view of electret and electrodes in the dual-phase arrangement [11] is shown in Fig. 5b.

NON-LINEAR SPRING RESPONSE

The mechanical response of the spring-mass system is examined. The Si substrate is fixed on an

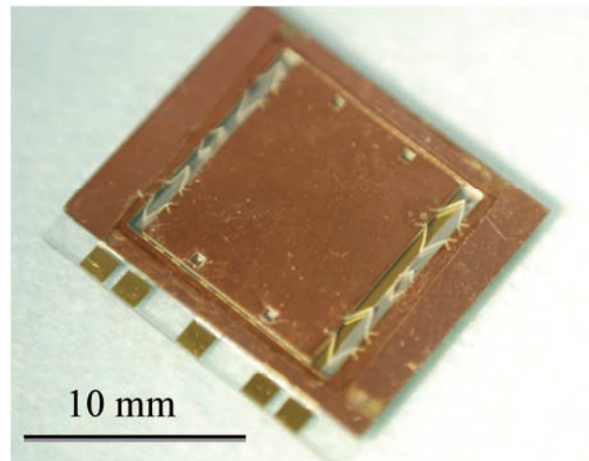


Figure 3. MEMS electret generator prototype with a nonlinear spring system.

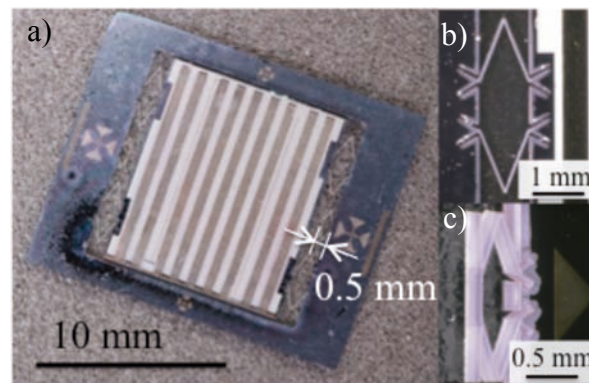


Figure 4. Backside of the top Si substrate. a) Overview, b) Parylene rhomboidal spring, c) Fixed-free secondary parylene spring.

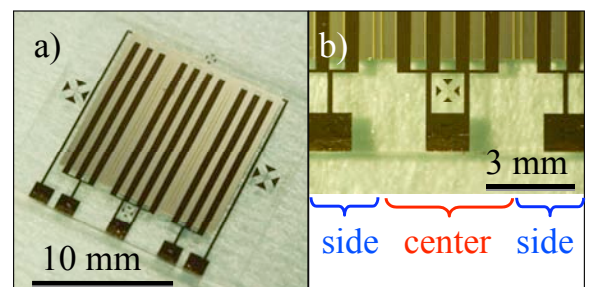


Figure 5. Bottom Pyrex substrate. a) Overview, b) Magnified view of electret and electrodes in the dual-phase arrangement.

electromagnetic shaker (APS-113, APS Dynamics), and shaken in the in-plane direction at prescribed frequency and amplitude. The relative displacement of the Si mass to the substrate is optically measured using a CCD camera. Figure 6 shows the frequency response of the Si mass. When the external oscillation amplitude is relatively small at 80 $\mu\text{m}_{\text{p-p}}$, maximum amplitude of 0.26 $\text{mm}_{\text{p-p}}$ is obtained at 45 Hz, which corresponds the resonant frequency of the main spring system. On the other hand, when the

external amplitude becomes larger than $200 \mu\text{m}_{p-p}$, the secondary spring is engaged, and the spring systems exhibit nonlinear behavior. Thus, amplitude over 1.0 mm_{p-p} is obtained in a broad frequency range of 46-73 Hz (Fig. 7). The amplitude is abruptly reduced when the frequency is increased to 74 Hz. The amplitude response has hysteresis depending on the direction of varying the frequency. These behaviors are typically seen in nonlinear spring systems such as a hardening spring.

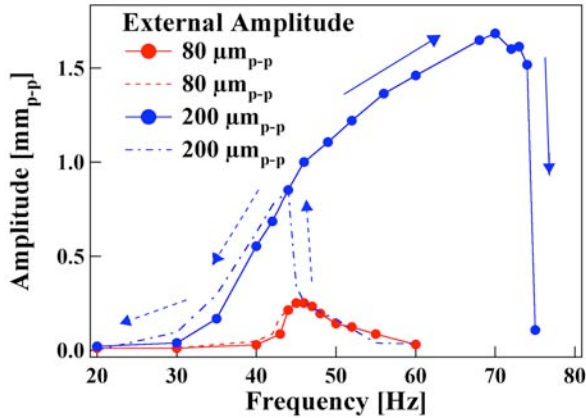


Figure 6. Frequency response of the mass-spring system.

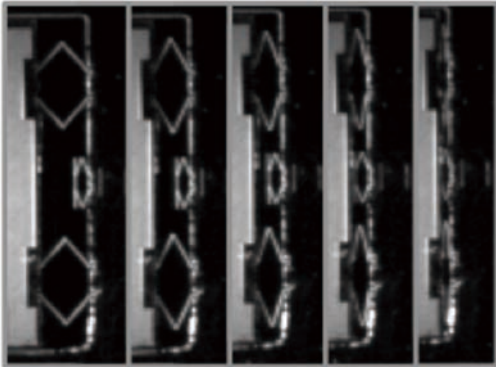


Figure 7. Snap shots of the hybrid spring systems.

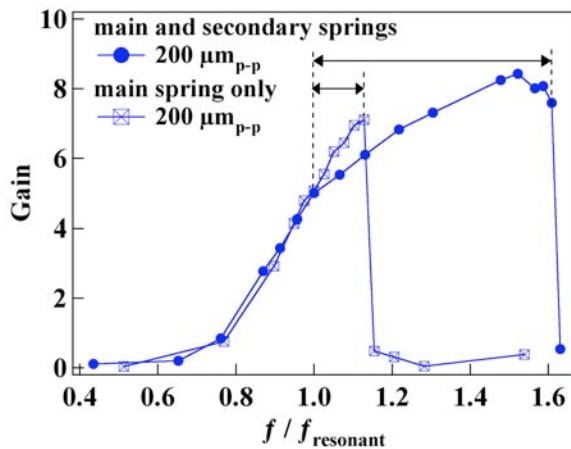


Figure 8. Gain (amplitude ratio) versus frequency ratio. External oscillation amplitude is $200 \mu\text{m}_{p-p}$. The secondary spring is engaged for gain >5 .

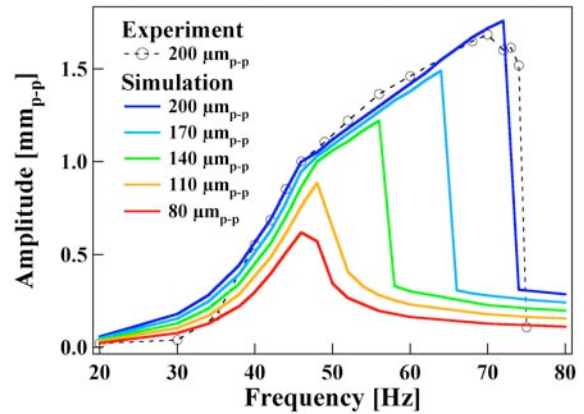


Figure 9. Simulation results of frequency response with different oscillation amplitude. Experimental data is also plotted at the oscillation amplitude of $200 \mu\text{m}_{p-p}$.

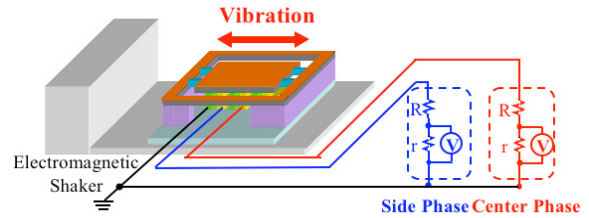


Figure 10. Experimental setup of power generation.

Figure 8 shows gain versus frequency ratio under the external oscillation amplitude of $200 \mu\text{m}_{p-p}$. Without the secondary spring, the gain becomes large only near the resonant frequency. On the other hand, frequency range with large amplitude becomes much broader with the secondary spring. Therefore, the nonlinear behavior of the spring enables operation with large amplitude in broader frequency range.

Simulation results for different external oscillation amplitude are shown in Fig. 9. The equation of motion is solved with a nonlinear spring of which characteristic is determined by curve fitting of the data shown in Fig. 6. When the external oscillation amplitude is increased, the frequency range with large amplitude becomes broader. Therefore, optimal design of the spring system including the secondary spring is necessary under given operation condition.

POWER GENERATION EXPERIMENT

In order to examine the power output of the electret generator presently developed, the generator is fixed on the shaker, and is oscillated in the in-plane direction at a frequency of 63 Hz as shown in Fig. 10. Figure 11 shows power output versus the external load at 63 Hz with the acceleration of 2 G, where purely resistive load is employed. The output power of the center phase is $0.56 \mu\text{W}$, and that of the side phase is $0.48 \mu\text{W}$, corresponding to the total

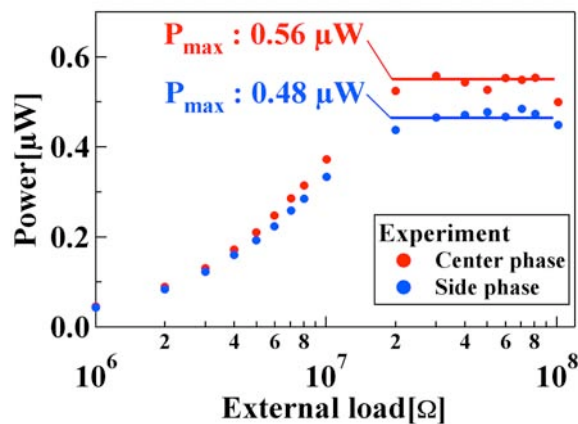


Figure 11. Power output versus external load at an input acceleration of 2 G with 63 Hz.

power output of 1.0 μW . The present data near the matched impedance are leveled off. This is probably because the damping force becomes large near the matched impedance, and the amplitude of mass is reduced. Another possibility is change of the air gap for different external load. Further investigation is required to explain this discrepancy. Note that, surface potential of the CYTOP electrets in this prototype is estimated to be as low as -180 V . With higher surface potential and smaller air gap, we can expect power output more than $10\ \mu\text{W}$ can be achieved at 1 G with the present configuration.

CONCLUSION

We have developed a MEMS in-plane electret generator with parylene high-aspect-ratio spring for energy harvesting applications. Nonlinear hybrid spring system with a secondary spring is designed to broaden the frequency range with large amplitude. Large amplitude of $1.0\text{ mm}_{\text{p-p}}$ has been obtained at a broad frequency range of 46-73 Hz. We have shown that numerical model of the nonlinear spring can mimic frequency response of the actual mass-spring system. With the present prototype with a $70\ \mu\text{m}$ gap, about $0.5\ \mu\text{W}$ has been obtained for both phases of the generator, corresponding to the total power output of $1.0\ \mu\text{W}$ at 63 Hz with the acceleration of 2 G.

This work is supported by the New Energy and Industrial Technology Development Organization (NEDO) of Japan. Photomasks are made using the University of Tokyo VLSI Design and Education Center (VDEC)'s 8-inch EB writer F5112+VD01 donated by ADVANTEST Corporation.

REFERENCES

- [1] J. A. Paradiso, and T. Starner, "Energy scavenging for mobile and wireless electronics," *IEEE Pervasive Comp.*, Vol. 4, pp. 18-27, 2005.
- [2] S. P. Beeby, M. J. Tudor, and N. M. White, "Energy harvesting vibration sources for micro systems applications," *Meas. Sci. Technol.*, Vol. 17, pp.175-195, 2006.
- [3] J. Borland, Y.-H. Chao, Y. Suzuki, and Y.-C. Tai, "Micro electret power generator," *Proc. 16th IEEE Int. Conf. MEMS*, Kyoto, pp. 538-541, 2003.
- [4] T. Tsutsumino, Y. Suzuki, N. Kasagi, and Y. Sakane, "Seismic power generator using high-performance polymer electret," *Proc. 19th IEEE Int. Conf. MEMS*, Istanbul, pp. 98-101, 2006.
- [5] Y. Naruse, N. Matsubara, K. Mabuchi, M. Izumi, and S. Suzuki, "Electrostatic micro power generator from low frequency vibration such as human motion," *J. Micromech. Microeng.*, Vol. 19, 094002, 5pp, 2009
- [6] H.-W. Lo, and Y.-C. Tai, "Parylene-based electret power generators," *J. Micromech. Microeng.*, Vol. 18, 104006, 8pp, 2008.
- [7] Y. Sakane, Y. Suzuki, and N. Kasagi, "Development of high-performance perfluorinated polymer electret film and its application to micro power generation," *J. Micromech. Microeng.*, Vol. 18, 104011, 6pp, 2008.
- [8] M. Edamoto, Y. Suzuki, N. Kasagi, K. Kashiwagi, Y. Morizawa, T. Yokoyama, T. Seki, and M. Oba, "Low-resonant-frequency micro electret generator for energy harvesting application", *Proc. 22nd IEEE Int. Conf. MEMS*, Sorrento, pp. 1059-1062, 2009.
- [9] Y. Suzuki, and Y.-C. Tai, "Micromachined high- aspect-ratio parylene spring and its application to low-frequency accelerometers," *J. Microelectromech. Syst.*, Vol. 15, pp.1364-1370, 2006.
- [10] Y. Tsurumi, Y. Suzuki, and N. Kasagi, "Non-contact electrostatic micro-bearing using polymer electret," *Proc. 21th IEEE Int. Conf. MEMS*, Tucson, pp. 511-514, 2008.
- [11] D. Miki, Y. Suzuki, and N. Kasagi, "Effect of nonlinear external circuit on electrostatic damping force of micro electret generator," *Proc. Transducers '09*, Denver, pp. 636-639, 2009.